

Image Dedusting with Deep Learning based Closed-Loop Network

Xibin Song¹, Liangjun Zhang¹, Dingfu Zhou¹ and Jin Fang¹

¹Robotics and Autonomous Driving Laboratory, Baidu Research, China

{songxibin, liangjunzhang, zhoudingfu, fangjin}@baidu.com

Abstract -

Computer vision technologies, including 2D/3D perceptions, have grasped more and more attentions in construction industry, which can provide effective support in many industry tasks, including autonomous digging and safety protection. However, dusts and mists always exist in many industry jobsites, which heavily affects the applications of computer vision technologies in industry operations, such as stone and truck detection and segmentation. To relief these problems, we propose a dedusting approach that utilizes deep convolutional network based closed-loop framework to remove the influence of dust and mist in construction sites. Taking an image with dust as input, the proposed framework can effectively remove the dust component, thus clean image can be obtained.

To achieve this, we divide the image with dust into three components, including clean image component, atmospheric light component and transmission (dust) component, and a U-Net structure that contains an encoder and three decoders is used, where the encoder is for effective feature extraction, and the three decoders are for the recovery of the three image components, thus clean image, atmospheric light and transmission (dust) components can be obtained. To guarantee that the network can be convergent, two supervisions are utilized, one for the clean image, and the sum of the three image components should be same with the input. Experiments demonstrate the effectiveness of the proposed approach.

Keywords -

Dedust; Deep Learning; Closed-Loop; Computer vision

1 Introduction

Computer vision technologies have drawn more and more attentions in construction industry, because complementary and effective information can be provided to improve the efficiency and safety in many industry jobsites, such as obstacle detection [1], segmentation [2] and depth enhancement [3][4][5], *etc.* However, bad weather events such as fog, mist and haze may exist in the construction industry, besides, dust also commonly occurs in the process of industry job, which dramatically reduce the visibility of many scenery and constitute significant obstacles. While images captured from hazy and dust fields usually preserve most of their major context, they require some visibility enhancement as a pre-processing before feeding them into computer vision algorithms. This pre-processing is generally called as image dehazing/dedusting, and image dehazing/dedusting techniques aim to generate haze and dust free images purified from the bad weather and dust



Figure 1. Example images captured in hazy and dust environment. (a) Hazy images and (b) Dust images.

environment events.

Sample hazy and dust images are illustrated in Fig. 1 (a) and (b), respectively. These images are captured under heavy hazy and dust conditions, where the objects, such as trees, excavators and roads are hard to identify, and the performances of computer vision technologies are limited under such conditions. To relief the influence of hazy and dust, single image dehazing methods have been proposed which dehaze an input image without requiring any extra information. Single image dehazing approaches are divided into prior information-based methods and learning based methods. Prior information-based methods are mainly based on the parameter estimation of atmospheric scattering model by utilizing the priors, such as dark channel priors, color attenuation prior and hazeline prior. Meanwhile, except the network structures, the performance of deep learning based approaches also rely on training data, and researchers tend to create synthetic dehazing datasets, which have a more practical creation process than real dehazing datasets.

According to previous approaches [6], hazy and dust

images contains three components, including transmission map, clean image and atmospheric light. The transmission map means the hazy/dust component, the atmospheric light means the atmosphere of the sky and the clean image is the target image that aims to recover. Most of current deep learning based approaches usually takes hazy and dust images as input and directly regress the clean images with direct supervision. In this paper, we propose a novel network which utilizes a closed-loop framework to effectively recover clean images using hazy/dust images as input. In specific, the proposed framework employs a U-Net structure which contains an encoder and three decoders, where the encoder aims to extract effective features, and the three decoders aim to recover the three image components of the hazy/dust images. Meanwhile, to guarantee that the network can be convergent, two losses are utilized. Firstly, clean loss: the recovered clean image should be same with groundtruth, which is the first loss. Secondly, reconstruction loss: the recovered transmission map, clean image and atmospheric light should reconstruct the hazy/dust images (input images) if the network works well, which means the closed-loop. The contributions of this paper can be summarized as:

- We propose a novel framework which contains a closed-loop structure and can recover the transmission map, clean image and atmospheric light of the hazy/dust images, simultaneously.
- Two losses, named clean and reconstruction loss, are utilized, which guarantees that the proposed framework can be convergent.
- Experiments demonstrate that hazy/dust images can be well tackled which prove the effectiveness of the proposed approach.

The remainder of this paper is organized as follows: related works are reviewed in Section 2, the proposed method is introduced in Section 3, the experiments and results at the actual site are described in Section 4, and the conclusions are presented in Section 5.

2 Related work

Currently approaches are mainly focus on image dehazing, which is divided into hand-crafted prior based and learning-based data-driven solutions.

2.1 Handcrafted Prior based Image Dehazing

Single image dehazing is an ill-posed problem in computer vision, and prior based approaches have been proposed to relief the problem. [7] proposes the dark channel prior (DCP) based approach, which is based on the observation that local regions in natural non-hazy scenes have

very low intensity in at least one of their color channels. The pixel values in the dark channel increases with haze increases. Thus, the value in the dark channel can be used to measure haze component and transmission map. Several techniques refined the DCP for halo free transmission map estimation using different edge-preserving smoothing filters. Except the dark channel prior, color-lines, color attenuation prior, color ellipsoidal prior, gamma correction prior, haze-lines also commonly used in image dehazing.

Meanwhile, previous approaches have proven that hazy images are prone to color cast issues in the presence of different atmospheric conditions like the sandstorm. Based on the observation, haze density weight along with white balancing for haze aware is utilized in image dehazing [8]. Besides, saturation correction that handles color cast is also proposed in image dehazing [9]. Furthermore, [10] proposes saturation-based transmission map estimation for dehazing which performs color correction using white balancing approach.

2.2 Learning based Image Dehazing

Deep learning based approaches have also proven the effectiveness in image dehazing. DehazeNet [11] proposes effective strategy to estimate the transmission map for image dehazing. Meanwhile, DCPDN [12] proposes a dense encoder-decoder model to effectively estimate the transmission map and atmospheric light, thus clean images can be obtained. Considering the image-to-image translation over the atmospheric model expression for image dehazing, [13] proposes a generative adversarial network (GAN) based Pix2pix network to recover clean images. Besides, [14] proposes GAN based model for dehazed texture-aware image dehazing, which comprises of CycleGAN and conditional GAN. In [15], the effectiveness of patch size is analysed in DCP based image dehazing approaches, and an efficient patch map selection mechanism is utilized through CNN for clean image recovery. Meanwhile, a gradient prior is utilized in [16] which combines the idea of DCP with a semi-supervised deep model to obtain clean images. GridDNet [17] introduces an end-to-end deep learning architecture with pre- and post-processing blocks to obtain clean images with hazing image as input. Multi-scale CNNs is also employed in [18] for image dehazing, and [19] produces haze-free images using multi-scale gated fusion network using encoder-decoder architecture. What's more, in RYF-Net [20], RNet, YNet and FNet are utilized for transmission map estimation in RGB and YCbCr space, respectively, thus clean images can be obtained with the estimated transmission maps. To well perform image dehazing, FAMED-Net [21] proposes a fast multi-scale dehazing model to fuse the response from a three scale encoder. [22] proposes to learn different levels of haze and develop an integration strategy to get the

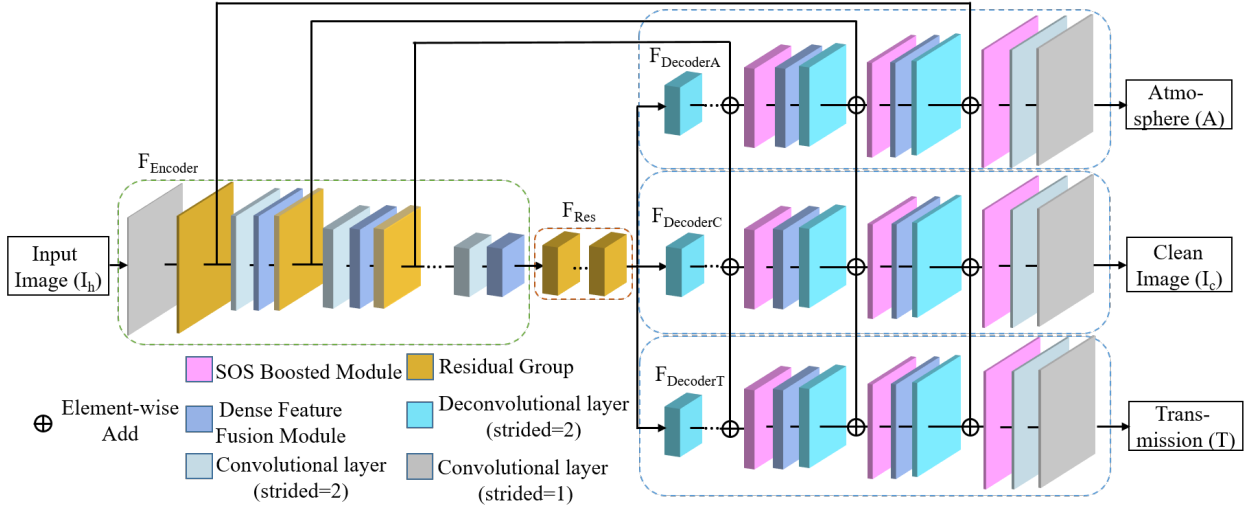


Figure 2. The figure demonstrates the network architecture of our approach. Using hazy/dust image as input, an encoder module and three decoders are used to recover atmospheric light (A), clean image (I_c) and transmission map (T) of the input image, respectively. $F_{Encoder}$ is first used to extract features, where Dense Feature Fusion strategy and Residual Group (F_{Res}) are utilized in the encoder process to obtain better features. In the decoder process ($F_{DecoderA}$, $F_{DecoderC}$ and $F_{DecoderT}$), deconvolutional layers are first used to up-sample the features, then SOS Boosted strategy is employed to enhance the obtained features. To obtain better results, the Dense Feature Fusion strategy are also used in the decoder process.

final dehazed images. Besides, [6] proposes a multi-scale based deep network which works on strengthen-operate-subtract-boosting strategy for image dehazing.

3 Our Approach

According to existing approaches [6], a hazy image I_h can be modeled as following:

$$I_h(x) = T(x)I_c(x) + (1 - T(x))A \quad (1)$$

where I_c denotes a haze-free clean image, A describes the global atmospheric light indicating the intensity of ambient light, T is the transmission map, and x represents the pixel position. Then, Eq. 1 can be reformulated as:

$$I_c(x) = \frac{I_h(x) - (1 - T(x))A}{T(x)} \quad (2)$$

Hence, the $I_c(x)$ can be obtained if transmission map T and atmospheric light A can be estimated. Besides, if I_c , T and A can be well recovered, the hazy image I_h can also be reconstructed. Based on Eq. 1 and Eq. 2, we propose an effective framework for image dehazing and dedusting.

In specific, the proposed network is based on the U-Net architecture, and the multi-scale boosted decoder (SOS boosting strategy) proposed in [6] is also utilized here. As shown in Fig. 2, the network includes three components, an encoder module ($F_{Encoder}$), a boosted decoder module ($F_{Decoder}$), and a feature restoration mod-

ule (F_{Res}). The boosted decoder module ($F_{Decoder}$) contains three decoders, including $F_{DecoderA}$, $F_{DecoderC}$ and $F_{DecoderT}$, which are designed for the estimation of Atmospheric light, clean image and Transmission map, respectively. Using a hazing/dusting image as input, the proposed framework can obtain the Atmospheric light, clean image and Transmission map, simultaneously. Specifically, SOS boosting strategy, dense feature fusion and residual group are used in the encoder and decoder processes.

3.1 Residual Group

Following [6], the residual structure is used in this paper, which aims to intensify the features using a residual mechanism. A residual block contains a Conv-ReLU-Conv structure and a addition operation, and the residual group contains K residual blocks. In this paper, we set $K = 3$.

3.2 Boosting Strategy

The effectiveness of boosting strategy has been proven in image denoising. Using the previously estimated image, [6] uses SOS boosting algorithm as a refinement process to obtain the strengthened image. The algorithm works positively to improve the Signal-to-Noise Ratio (SNR) under the axiom, and the denoising method with boosting strategy obtains better results in terms of SNR with less noise. For image dehazing, the SOS boosting

strategy can be formulated similarly as:

$$\hat{J}^b = g(I + \hat{J}) - \hat{J} \quad (3)$$

where \hat{J}^b denotes the estimated image after boosting strategy, and $g(\cdot)$ is the dehazing approach, and $I + \hat{J}$ represents the strengthened image using the hazy input I . Following [6] and as shown in Fig. 2, we also utilize boosting strategy to obtain better dehazing/dedusting image results in this paper, and please see [6] for more details.

3.3 Dense Feature Fusion Module

The U-Net architecture is commonly used, and several drawbacks are exists, including: (1) the spatial information is missed in the process of the encoder block, and (2) the connections between the features from non-adjacent levels are insufficient. In this paper, to remedy the missing spatial information and exploit the features from non-adjacent levels, the Dense Feature Fusion Module (DFF) is used here. Following [6], the DFF aims to intensify the boosted features using an error feedback mechanism, which is used in both the encoder and the decoder blocks. As shown in Fig. 2, two DFF modules are utilized in both the encoding and decoding processes. In specific, one of the DFF module is used before the residual group in the encoder and another DFF module is used after the SOS boosted module in the decoder. Besides, feature fusion is also employed by connecting the enhanced DFF output in the encoder/decoder to obtain more representative features.

3.4 Loss

As discussed above, using the hazing/dusting image I_h as input, the proposed framework can obtain the Atmospheric light (A), clean image (I_c) and Transmission map (T), simultaneously, and the estimated A , I_c and T can be used to reconstruct the input hazing/dusting image, which means the closed-loop. Hence, two losses, including clean loss ($loss_c$) and reconstruction loss ($loss_r$) with L1 are utilized, which can be formulated as:

$$loss_c = \sum \|I_{gt} - I_c\| \quad (4)$$

where I_{gt} means the groundtruth clean image, I_c means the estimated dehazing/dedusting images obtained by our approach.

$$loss_r = \sum \|I_h - \hat{I}_h\| \quad (5)$$

I_h means the input image and \hat{I}_h means the reconstructed input image using estimated A , I_c and T with $\hat{I}_h = TI_c + (1 - T)A$.

The final loss is defined as:

$$loss = \alpha loss_c + \beta loss_r \quad (6)$$

where α and β are weight parameters and we set $\alpha = 0.5$, $\beta = 0.5$ empirically in this paper.

3.5 Implementations

In this section, we provide more implementation details of our approach. In specific, as shown in Fig. 2, in each decoder module ($F_{DecoderA}$, $F_{DecoderC}$ and $F_{DecoderT}$), convolutional and deconvolutional layers are used in this paper. And after each convolutional and deconvolutional layer, the Leaky Rectified Linear Unit (LReLU) with a negative slope of 0.2 is used. For the residual group [23], it consists of three residual blocks in (F_{Res}). In the encoder module, the kernel size of the first layer is set as 11×11 pixels, and kernel size with 3×3 is set in all the other convolutional and deconvolutional layers. The proposed framework is jointly trained and the Mean Squared Error (MSE) is utilized as the loss function to constrain the network output and ground truth. ADAM solver [24] is employed and the entire training process contains 100 epochs. We set $\beta_1 = 0.9$ and $\beta_2 = 0.999$ with a batch size of 16. The initial learning rate is set as 104 with a decay rate of 0.75 after every 10 epochs.

3.6 Evaluation metrics

To effective demonstrates the effectiveness of our approach, following [6], two kind of evaluation metrics are employed here, including PSNR and SSIM.

Given two images I_x and I_y with pixel values from 0 to 255, the formulation of PSNR is defined as:

$$MSE = \frac{1}{MN} \sum_{i=0}^{M-1} \sum_{j=0}^{N-1} (I_x(i, j) - I_y(i, j))^2 \quad (7)$$

$$PSNR = 10 \log_{10} \left(\frac{255^2}{MSE} \right)$$

where M and N are the height and width of I_x and I_y .

The structural similarity index measure (SSIM) is used for measuring the similarity between two images (I_x and I_y). And the formulation of SSIM is defined as:

$$SSIM = \frac{(2\mu_x\mu_y + c_1)(2\delta_{xy} + c_2)}{(\mu_x^2 + \mu_y^2 + c_1)(\delta_x^2 + \delta_y^2 + c_2)} \quad (8)$$

where μ_x and μ_y are the averages of I_x and I_y , δ_x and δ_y are variances of I_x and I_y , δ_{xy} is the covariance of I_x and I_y , c_1 and c_2 are two variables to stabilized the division with weak denominator.

4 Experiment

To prove the effectiveness of our approach, we provide the experiment results of our proposed dehazing/dedusting approaches in both qualitative and quantitative levels.



Figure 3. Visualization of dedusting results of real-world captured dust images. The first rows are the input dust images and the second rows are the results obtained by our approach. As shown in this figure, the input images are suffered from heavy dust and our approach can remove the dust effectively.

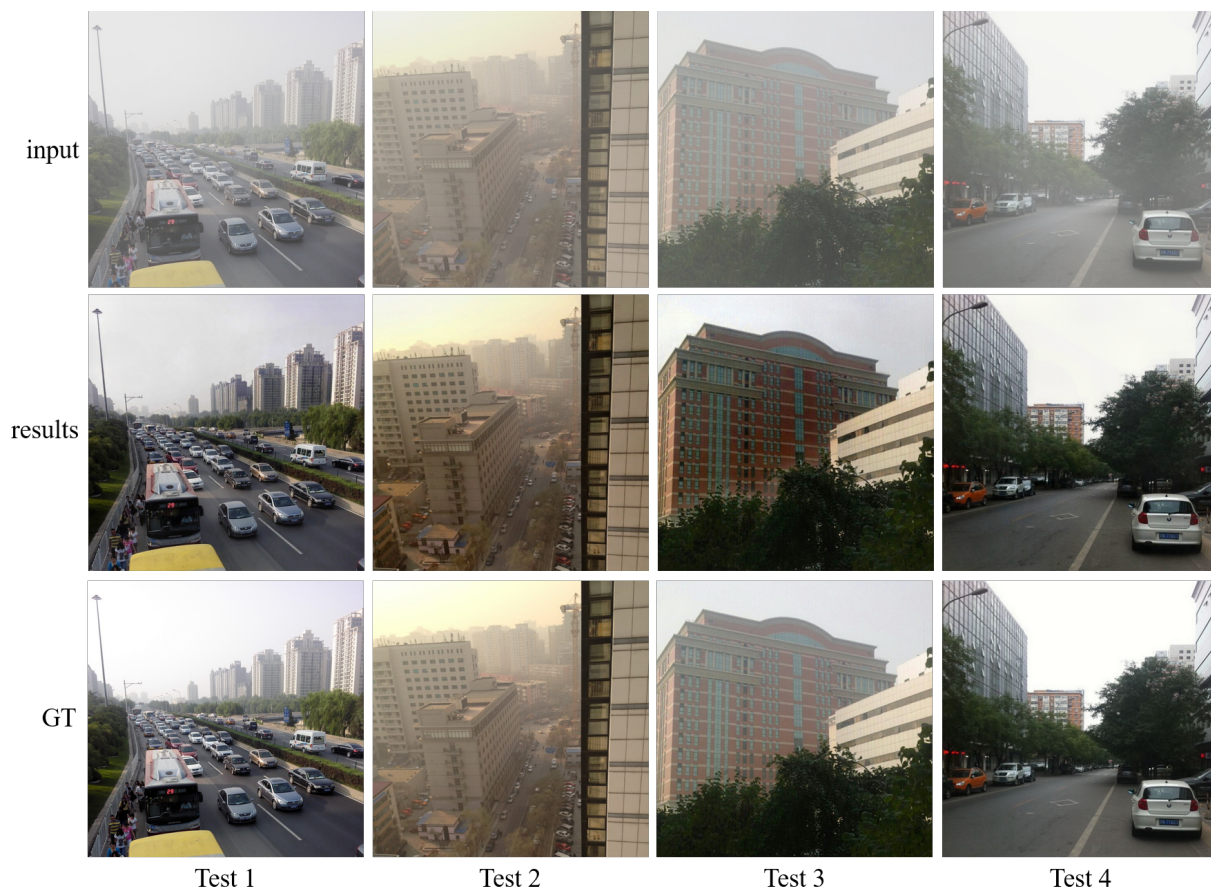


Figure 4. Visualization of dehazing results of hazy images generated in traffic scenarios. GT means ground truth images. The first row shows the input images, the second row shows the results obtained by our approach and the third row shows the ground truth images.

Following [6], the RESIDE dataset [25] is used as the training data for image dehazing. The RESIDE dataset [25] contains both synthesized and real-world hazy/clean image pairs for both indoor and outdoor scenes. Hence, to obtain a dehazing model with better generalization ability, 9000 outdoor hazy/clean image pairs from the RESIDE training dataset [25] are selected as the training set. Note that the redundant images from the same scenes are removed to avoid over-fitting the training process. To augment the training data, the images of each pair are resized with three random scales within the scale range from 0.5 to 1.0. Besides, to further augment the training images, the hazy images are randomly cropped with resolution of (256×256) patches and flip operation with horizontally and vertically directions are utilized here.

Meanwhile, for image dedusting, we use real-world captured dust/dust-free image pairs as the training dataset, and these images are captured under real-world industry operation scenarios. The training data for image dedusting model contains 1000 image pairs.

4.1 Dehazing/dedusting results

Fig. 3 and Fig. 4 illustrate the visualization results of image dedusting/dehazing, respectively.

Fig. 3 demonstrates a digging and truck loading process of an excavator, which is captured in a real-world industrial operation scenario. As shown in Fig. 3 (input), the digging and truck loading process is suffered with heavy dust, and the working areas and the excavator are blurry. In such process, the machine, such as excavator, is difficult to detect for human eyes due to the existed dust, and it is even harder to detect for computer vision technologies. Besides, the operation areas, such as the rock areas, are also difficult to localize, even for humans, which heavily impede the automation of such process. As shown in Fig. 3 (results), our approach can remove the influence of dust effectively, and the areas of excavator and rocks are easily found after the dedusting process.

Fig. 4 illustrates the dehazing results using hazy images captured in city scenes. As shown in Fig. 4 (input), hazy conditions are always exist in city and traffic scenes, which also heavily affect the detection and identification of buildings, cars and humans, etc. Besides, as shown in Fig. 4 (results), our approach can effectively remove the influence of hazy, and clean images can be obtained, which can help to detect and identify buildings, cars and humans, etc.

As shown in Fig. 3 and Fig. 4, our approach can effectively remove the dust and hazy components of dusting and hazing images, which can support the construction process in human working.

Table 1 and Table 2 demonstrate the quantitative results of PSNR and SSIM of the inputs and results obtained

Table 1. PSNR results of images shown in Fig. 4. The better results are shown in bold. "e-1d" mean results using one encoder and one decoder to recover clean images.

Eval	Test1	Test2	Test3	Test4
input	15.029	18.549	15.778	12.387
e-1d[6]	19.591	21.021	16.254	27.007
Our	20.035	21.411	16.620	27.501

Table 2. SSIM results of images shown in Fig. 4. The better results are shown in bold. "e-1d" mean results using one encoder and one decoder to recover clean images.

Eval	Test1	Test2	Test3	Test4
input	0.8041	0.8956	0.7845	0.7489
e-1d[6]	0.9207	0.9356	0.8525	0.9534
Our	0.9527	0.9603	0.8862	0.9707

by our approach. Test 1, Test 2, Test 3 and Test 4 in Table. 1 and Table. 2 mean the figures in Fig. 4. The PSNR and SSIM can be calculated with the formulation of Eq. 7 and Eq. 8. "e-1d" mean results obtained using one encoder-decoder structure [6], and "Our" mean results obtained using one encoder and three decoders with clean and reconstruction loss.

As shown in Table. 1, the PSNR results of our approach outperform the input images and "e-1d", which also prove that our approach can effectively remove the influence of hazy and recover better images that are close to the groundtruth. SSIM can be used for measuring the structure similarity between the recovered image and groundtruth. In Table. 2, better SSIM results can also be obtained by our approach, which prove that images with better structures can be obtained that are much more similar with the groundtruth.

5 Conclusion

In this study, we propose a closed-loop framework to remove the influence of dust and hazy in construction sites, which contains one encoder and three decoders. Taking a image with dust as input, the proposed framework can effectively remove the dust component, thus clean image can be obtained. To achieve this, we divide the image with dust into three components, including clean image component, atmospheric light component and transmission component, and a U-Net structure that contains a encoder and three decoders is used, where the encoder is for effective feature extraction, and the three decoders are for the recovery of the three image components, thus clean image, atmospheric light and transmission components can be obtained. Clean and reconstruction losses are utilized to guarantee that the network can be convergent. Experiments demonstrate the effectiveness of the proposed approach.

References

- [1] Kai Chen, Jiaqi Wang, Jiangmiao Pang, Yuhang Cao, Yu Xiong, Xiaoxiao Li, Shuyang Sun, Wansen Feng, Ziwei Liu, Jiarui Xu, et al. Mmdetection: Open mmlab detection toolbox and benchmark. *arXiv preprint arXiv:1906.07155*, 2019.
- [2] Shervin Minaee, Yuri Y Boykov, Fatih Porikli, Antonio J Plaza, Nasser Kehtarnavaz, and Demetri Terzopoulos. Image segmentation using deep learning: A survey. *IEEE Transactions on Pattern Analysis and Machine Intelligence*, 2021.
- [3] Xibin Song, Wei Li, Dingfu Zhou, Yuchao Dai, Jin Fang, Hongdong Li, and Liangjun Zhang. Mldanet: Multi-level dual attention-based network for self-supervised monocular depth estimation. *IEEE Transactions on Image Processing*, 30:4691–4705, 2021.
- [4] Xibin Song, Jianmin Zheng, Fan Zhong, and Xueying Qin. Modeling deviations of rgb-d cameras for accurate depth map and color image registration. *Multimedia Tools and Applications*, 77(12):14951–14977, 2018.
- [5] Xibin Song, Yuchao Dai, Dingfu Zhou, Liu Liu, Wei Li, Hongdong Li, and Ruigang Yang. Channel attention based iterative residual learning for depth map super-resolution. In *Proceedings of the IEEE/CVF Conference on Computer Vision and Pattern Recognition*, pages 5631–5640, 2020.
- [6] Hang Dong, Jinshan Pan, Lei Xiang, Zhe Hu, Xinyi Zhang, Fei Wang, and Ming-Hsuan Yang. Multi-scale boosted dehazing network with dense feature fusion. In *Proceedings of the IEEE/CVF Conference on Computer Vision and Pattern Recognition*, pages 2157–2167, 2020.
- [7] Kaiming He, Jian Sun, and Xiaoou Tang. Single image haze removal using dark channel prior. *IEEE transactions on pattern analysis and machine intelligence*, 33(12):2341–2353, 2010.
- [8] Lark Kwon Choi, Jaehee You, and Alan Conrad Bovik. Referenceless prediction of perceptual fog density and perceptual image defogging. *IEEE Transactions on Image Processing*, 24(11):3888–3901, 2015.
- [9] Yan-Tsung Peng, Zhihui Lu, Fan-Chieh Cheng, Yalun Zheng, and Shih-Chia Huang. Image haze removal using airlight white correction, local light filter, and aerial perspective prior. *IEEE Transactions on Circuits and Systems for Video Technology*, 30(5):1385–1395, 2019.
- [10] Se Eun Kim, Tae Hee Park, and Il Kyu Eom. Fast single image dehazing using saturation based transmission map estimation. *IEEE Transactions on Image Processing*, 29:1985–1998, 2019.
- [11] Bolun Cai, Xiangmin Xu, Kui Jia, Chunmei Qing, and Dacheng Tao. Dehazenet: An end-to-end system for single image haze removal. *IEEE Transactions on Image Processing*, 25(11):5187–5198, 2016.
- [12] He Zhang and Vishal M Patel. Densely connected pyramid dehazing network. In *Proceedings of the IEEE conference on computer vision and pattern recognition*, pages 3194–3203, 2018.
- [13] Yanyun Qu, Yizi Chen, Jingying Huang, and Yuan Xie. Enhanced pix2pix dehazing network. In *Proceedings of the IEEE/CVF Conference on Computer Vision and Pattern Recognition*, pages 8160–8168, 2019.
- [14] Jaihyun Park, David K Han, and Hanseok Ko. Fusion of heterogeneous adversarial networks for single image dehazing. *IEEE Transactions on Image Processing*, 29:4721–4732, 2020.
- [15] Wei-Ting Chen, Jian-Jiun Ding, and Sy-Yen Kuo. Pms-net: Robust haze removal based on patch map for single images. In *Proceedings of the IEEE/CVF Conference on Computer Vision and Pattern Recognition*, pages 11681–11689, 2019.
- [16] Lerenhan Li, Yunlong Dong, Wenqi Ren, Jinshan Pan, Changxin Gao, Nong Sang, and Ming-Hsuan Yang. Semi-supervised image dehazing. *IEEE Transactions on Image Processing*, 29:2766–2779, 2019.
- [17] Xiaohong Liu, Yongrui Ma, Zhihao Shi, and Jun Chen. Griddehazenet: Attention-based multi-scale network for image dehazing. In *Proceedings of the IEEE/CVF International Conference on Computer Vision*, pages 7314–7323, 2019.
- [18] Wenqi Ren, Si Liu, Hua Zhang, Jinshan Pan, Xiaochun Cao, and Ming-Hsuan Yang. Single image dehazing via multi-scale convolutional neural networks. In *European conference on computer vision*, pages 154–169. Springer, 2016.
- [19] Wenqi Ren, Lin Ma, Jiawei Zhang, Jinshan Pan, Xiaochun Cao, Wei Liu, and Ming-Hsuan Yang. Gated fusion network for single image dehazing. In *Proceedings of the IEEE Conference on Computer Vision and Pattern Recognition*, pages 3253–3261, 2018.

- [20] Akshay Dudhane and Subrahmanyam Murala. Ryf-net: Deep fusion network for single image haze removal. *IEEE Transactions on Image Processing*, 29: 628–640, 2019.
- [21] Jing Zhang and Dacheng Tao. Famed-net: A fast and accurate multi-scale end-to-end dehazing network. *IEEE Transactions on Image Processing*, 29:72–84, 2019.
- [22] Yunan Li, Qiguang Miao, Wanli Ouyang, Zhenxin Ma, Huijuan Fang, Chao Dong, and Yining Quan. Lap-net: Level-aware progressive network for image dehazing. In *Proceedings of the IEEE/CVF International Conference on Computer Vision*, pages 3276–3285, 2019.
- [23] Bee Lim, Sanghyun Son, Heewon Kim, Seungjun Nah, and Kyoung Mu Lee. Enhanced deep residual networks for single image super-resolution. In *Proceedings of the IEEE conference on computer vision and pattern recognition workshops*, pages 136–144, 2017.
- [24] Diederik P Kingma and Jimmy Ba. Adam: A method for stochastic optimization. *arXiv preprint arXiv:1412.6980*, 2014.
- [25] Boyi Li, Wenqi Ren, Dengpan Fu, Dacheng Tao, Dan Feng, Wenjun Zeng, and Zhangyang Wang. Re-side: A benchmark for single image dehazing. *arXiv preprint arXiv:1712.04143*, 1, 2017.